Nauw, J.; Philippart, C.J.M.; Duran-Matute, M. & Gerkema, T. (2017). Estimates of exposure times in the Wadden Sea : A comparison of methods. *Journal of Sea Research*, 127, 12-25

Published version: https://dx.doi.org/10.1016/j.seares.2017.03.015

Link NIOZ Repository: www.vliz.be/nl/imis?module=ref&refid=289565

Estimates of exposure times in the Wadden Sea: a comparison of methods

Janine Nauw[1], Catharina J.M. Philippart[1], Matias Duran-Matute[2,3], Theo Gerkema[3,]

[1] NIOZ Netherlands Institute for Sea Research, Department of Coastal Systems, and Utrecht University, PO Box 59 1790 AB Den Burg, The Netherlands

E-mail: Janine@Nauw.xs4all.nl, Katja.Philippart@nioz.nl

[2] Eindhoven University of Technology, Eindhoven, the Netherlands.

Email: m.duran.matute@tue.nl

[3] NIOZ Netherlands Institute for Sea Research, Department of Estuarine and Delta Systems, and Utrecht University, PO Box 140, 4400 AC Yerseke, The Netherlands

E-mail: Theo.Gerkema@nioz.nl

Keywords: *exposure times, GETM, Dutch Wadden Sea*

ABSTRACT

In this study, we have compared three methods to determine the exposure times of intertidal flats in the Dutch Wadden Sea. The first method was based on a triangulation (TRIA) of the sea level elevations measured at the tidal gauges surrounding the Dutch Wadden Sea, following Rappoldt *et al.* (2004); for the second, method numerical simulations with the General Estuarine Transport Model (GETM) were used, and the third method (HYBRID) is a combination of the previous two. The first two methods show a good agreement for the western Dutch Wadden Sea, an area

where the density of intertidal flats is low. However, the results of TRIA and GETM show differences of as much as 20% for the much shallower eastern part of the Dutch Wadden Sea.

To explore the influence of the number and distribution of tidal gauge stations on these differences, virtual tidal gauges were added to the existing network of tidal gauge stations, based on model results. An analysis showed that there is limited added value to an even large (three-fold) increase in the number of tide gauges, largely because of the highly non-linear behavior of the tidal wave in the model compared to the linear approach adopted in the triangulation method.

The third approach (HYBRID) was developed by combining the previous two methods. Tidal prediction was obtained from applying a Least Squares Harmonic Analysis on the Sea Level Height (SLH) in the simulation with GETM at every grid point. Moreover, the unpredictable part, e.g. the set-ups or set-downs induced by winds from the North Sea or the European continent, was determined by applying the triangulation method to the wind-induced SLH observed at the tidal gauge stations. This wind-induced SLH was defined as the observed sea level height minus the tidal prediction and its long-term mean value. This combination of methods offers a new approach to determine exposure times in the Wadden Sea more accurately than either method individually.

1. INTRODUCTION

The Wadden Sea is the largest natural reserve in the Netherlands extending further along the German Bight all the way to Denmark. Due to its Outstanding Universal Value, it became a UNESCO world heritage site. The Wadden Sea is bounded by the mainland on one side and by a chain of barrier islands that separates it from the North Sea on the other. Inlets between the barrier islands allow for an exchange of water, nutrients and sediments with the North Sea. The bathymetry of the Wadden Sea shows deep tidal gullies surrounded by intertidal flats.

The tidal wave in the North Sea progresses from the south along the Dutch coast into the German

Bight; as it passes, it subsequently enters the Wadden Sea through each of the inlets. The tide thus causes alternate flooding and drying of the intertidal flats. As the tide has a distinct semi-diurnal character in The Dutch Wadden Sea, the intertidal flats are flooded twice per day. Importantly, the inundation and exposure times are affected not only by tides but also by wind surges and depressions, which makes the phenomenon more irregular and less predictable. We call the duration, during which an intertidal flat is flooded, the inundation or immersion time. Conversely, the time, when it is exposed to the air, is called the exposure or emersion time. We will express the inundation and exposure times as a percentage or fraction of the total time.

The exposure time plays a key role in many biological processes. For example, growth of microphytobenthos, microcopic benthic algae that live in the top layer of the sediment of intertidal flats, can only grow if light levels are sufficiently high [1]. Because suspension-feeding benthic fauna such as mussels, cockles and oysters can only graze on phytoplankton (pelagic microscopic algae) if the tidal flats are submerged, their abundances and growth rates are inversely proportional to the exposure time [2, 3, 4, 5, 6]. Submersion time also determines the susceptibility of benthic fauna to predation. Small cockles, for example, are vulnerable to predation by crabs when submerged, whereas larger cockles are being fed on by oystercatchers during exposure [7]. This implies that the carrying capacity of the Wadden Sea for benthos and benthos-feeding waders is strongly related to the area of tidal flats, which is determined by the combination of bathymetry and exposure time [8, 9]. Hence, it is important to have accurate spatio-temporal maps of exposure times in intertidal basins such as the Wadden Sea. In addition, the exact time of drying and flooding is also necessary to know when planning a field campaign to collect samples on tidal flats, such as SIBES [8]. So far, however, no accurate method to produce such maps have been developed.

In this study, we compare three different methods to estimate the exposure time of the intertidal flats in the Dutch Wadden Sea. The first method was based on a triangulation of the sea level elevations as measured at the tidal gauges surrounding the Dutch Wadden Sea as developed by [11]; whereas in the second method, numerical simulations with the General Estuarine Transport Model (GETM) were used. Both methods have their advantages and shortcomings. The third method (HYBRID) is a combination of the previous two.

The triangulation method (TRIA) uses *in-situ* observations, and therefore, it incorporates the effect of tides and storm surges in a direct and realistic way in the vicinity of the tidal gauges. Calculations are relatively fast and can be performed online (see "Intertides" at www.walterwaddenmonitor.org/en/tools/intertides/). However, the paucity of tidal gauges in the Wadden Sea leaves us with coarse interpolations across watersheds. This method is then unlikely to account properly for the tidal propagation and its complex pattern of phase differences, as the tide enters via different inlets at different moments.

The General Estuarine Transport Model (GETM), on the other hand, carefully determines the propagation of the tidal wave through the inlets into the Wadden Sea and thus accounts for the phase difference [15]. However, caveats arise from the way "drying" of tidal flats is modelled, e.g. "dry" in GETM means "below a certain threshold value". The values assumed for this threshold has significant impact on the exposure time and exposed area [12]. Additionally, the numerical model is quite expensive in terms of computational effort and requires realistic forcing data that are only available for certain years of the recent past.

After a description of the first two methods (including their differences in underlying information on bathymetry), estimates of exposure time by TRIA and GETM were compared in space and time. Because differences in the outcomes of both methods might be due to the number of tidal gauge stations, virtual tidal gauges were subsequently added to the existing network of tidal gauge stations and differences in sea level height variations recalculated.

A third method is proposed (HYBRID), combining the best of the two, and subsequently validated by means of field observations at pressure gauges on the Balgzand tidal flat and bootstrapping (i.e. comparing the prediction and actual sea level height at one tidal gauge based on a model using the information of all others).

Finally, the three models (TRIA, GETM and HYBRID) are discussed with regard to their accuracy and efficiency. Moreover, their applicability as operational method is discussed besides their use in gaining knowledge about ecosystems behavior.

2. MATERIAL AND METHODS

2.1 Triangulation method (TRIA)

In this method, developed by Rappoldt [11], a triangulation was applied to the tidal gauge data from 15 different stations in and around the Dutch Wadden Sea (live.waterbase.nl) of which two are located in the Ems estuary. Besides these 15 stations, Figure 1 also shows three tidal gauge stations in the North Sea that have not been incorporated in the initial analysis in [11], but will be used later in this study. The Sea Level Height (SLH) is recorded once every ten minutes at all gauges. Any combination of three stations defines a triangular plane, with its tilt and height changing in time with the level at its vertices (i.e. at the stations). The triangular plane can then be assumed to define the instantaneous water level at all locations within the triangle [11]. This is in effect a linear interpolation, which was carried out on a regular 20x20 m grid. Outside the area covered by triangles, linear extrapolation was applied using the nearest tidal gauge stations. This was done, for example, in the Balgzand tidal basin and the Ems estuary. Bathymetry at the 20x20 grid was derived from the "cycle 5" bathymetry described in [13]. All depths are given in comparison to the Amsterdam Ordnance Datum as a reference level. It is based mostly on the soundings performed by Rijkswaterstaat (RWS; www.rijkswaterstaat.nl) between 2006 and 2012. LIDAR data over the Groninger Wad (2007) and the coast of Texel (2009) were used to match data collected in different years. Missing data in the Balgzand area and between East-Vlieland and the mainland were filled with a smoothing procedure to fill the gaps. For details on the "cycle 5" bathymetry, we refer to [13] and for details on the triangulation method to [11].

The advantages of the triangular method are that it uses the widely available highly accurate *in-situ* observations of sea level height at the tidal gauge stations and that it is a very quick method with respect to calculation times. The disadvantage is that it is a linear method and therefore implicitly assumes that the tides behave linearly, even in shallow complex areas such as the eastern part of the Dutch Wadden Sea.

2.2 General Estuarine Transport Model method (GETM)

This method uses output from numerical simulations performed using the General Estuarine Transport Model (GETM, developed by [14]) applied to the Dutch Wadden Sea. In particular, we used output from the simulations described in [15]. GETM is a finite difference model solving the three-dimensional hydrostatic Navier-Stokes equations of motion with a turbulence closure scheme. The model bathymetry was based on the RWS sounding data between 2004 and 2012, at 20 m resolution, which was rotated 17^{o} with respected to the East-West axis and subsequently averaged over 10x10 points leading to a bathymetry at 200x200 m resolution. The bathymetric map was further smoothed for model stability. Boundary conditions for SLH, vertical integrated velocities and vertical profiles of temperature and salinity were applied at the open boundaries; meteorological data was obtained from the operational forecast model of the German Weather Service (DWD; www.dwd.de) for forcing at the surface; and fresh water discharges at the sluices in the model domain were imposed. In the vertical, 30 terrain following sigma layers were used. The model was run for three years: 2009 to 2011. Details on the model setup and validation of the results with measurements of SLH at the tidal gauge stations, salinity and temperature in the Marsdiep inlet, and water transport through the Texel inlet were given in [15].

GETM has a thin-layer flooding and drying algorithm, in which the total depth does not become less than a prescribed minimum depth, which was D_{min}=0.10 m in this simulation. Below a critical depth, D_{crit}=0.26 m, the bottom drag coefficient is increased exponentially for decreasing water depth and the influence of the non-linear terms is reduced to zero at the minimum depth, D_{min}. When this minimum depth is attained, the fluid becomes motionless and will therefore not contribute to the circulation in the rest of the domain. Locations with water depths such that $D \leq 0.26$ m are affected by the drying and flooding algorithm and, therefore, deviate from realistic water depths.

In post-processing of the numerical results from GETM, the local SLH pattern was determined from the total water depth, D, and the height of the bathymetry. At locations where the local water depth, D, was below the critical depth D_{crit} = 0.26 m, the SLH was disregarded and a more realistic value for the local SLH was determined by solving an elliptic PDE (Laplacian or Poisson's equation) on the SLHs surrounding the gap. This method leads to smooth SLH patterns including the tidal salt marsh areas close to the Dutch mainland. Artifacts are only observed near the eastern (open) boundary of the numerical domain, where the local water depth is small and ‘pools’ of water occur, trapping water at low tide. However, this area is not considered in the current paper. The critical depth in this numerical setup is sufficiently low that most of the interpolated SLHs eventually attain a value below the local bathymetry and hence are regarded as ‘dry’.

With the GETM method the advantages and disadvantages are exactly opposite to those of the TRIA method; the advantages are that this method takes into account the highly non-linear behavior of the tidal wave in shallow areas, but it is computationally costly and needs accurate forcing conditions for the period of interest. Moreover, the thin flooding and drying approach introduces an uncertainty in defining “exposure”.

3. RESULTS

3.1 Comparison of bathymetries

Exposure and/or immersion follow from the subtraction of the bathymetry from the Sea Level Height (SLH). Thus, besides the SLH itself, differences in the bathymetry may lead to differences in exposure time. The bathymetries used were both based on the sounding data (RWS), but in some areas (particularly in the eastern part) different years have been used. Moreover, additional processing was applied for the *cycle 5* bathymetry [13] to fill in missing data and improve connections between areas in which the data was collected in different years. We tested the compatibility of both sets. First, the *cycle 5* data and the original sounding data were compared, both at a resolution of 20x20 m. Large differences exist between these data (Figure 2 top panel), but careful examination of the results show that these were merely related to a shift in the underlying grid, which led to the misalignment of gullies and tidal flats and introduced large differences in areas with strong gradients in the bathymetry. The smallest difference between the data was obtained by shifting the grid of the cycle 5 data with (dx,dy)=(-10,-10) m (i.e. the bathymetry was shifted 10 m to the west and 10 m to the south and lower panel of Figure 2). However, that does not give an answer to which of the underlying grids was wrong. In any case, a mere shift of the grid does not influence the exposure times since the distance between the underlying grids is negligible compared to tidal wavelengths.

After shifting the grid, the large differences between both bathymetries at locations with strong gradients in the bathymetry cease to exist, and in 38% of the grid points, of which the bathymetry was unknown or marked as land, the difference was exactly zero. Large differences occur only in the Amelander Zeegat (tidal inlet between Terschelling and Ameland), and in the Friesche Zeegat (tidal inlet between Ameland and Schiermonnikoog). At both locations, the bathymetry changes significantly from year to year [16] especially at the outer delta. Therefore the differences were likely related to the bathymetry being from different years. The same holds for the Ems estuary, which also has a very dynamic bathymetry. In the rest of the Wadden Sea, the difference between the bathymetries was small and the overall mean absolute difference was 0.11 m. The accuracy of the soundings was estimated to be between 0.11 and 0.40 m [13, 17, 18], suggesting that the mean difference between the bathymetries falls within the error margin. Moreover, the focus of this study was not on the exposure time at the inlets, nor in the Ems-Dollard, which was not even included in the simulation with GETM, but on the intertidal flats inside the Wadden Sea, where differences are negligible.

3.2. Comparison of the exposure times between the individual methods

In the TRIA method, the SLH at all locations inside each triangle was determined by the triangulation of the sea level height at the corners of that particular triangle. This means that the

SLH can also be lower than the local height of the bathymetry; in the TRIA method these locations are marked “dry”. The simulated Sea Level Height (SLH) in GETM can never be lower than the local bathymetry due to the thin layer flooding and drying algorithm. In post-processing, the local water depth D (m) based on the SLH and the height of the bathymetry, was determined for each grid point every half hour. At locations where the local water depth D was below the critical depth D_{crit} = 0.26 m, the SLH was found by interpolation as explained in Section 3.2. Again, wherever the interpolated SLH was below the local height of the bathymetry, the point was marked dry.

The (relative) exposure time is defined as the percentage of the time that the SLH at a particular location is below the local height of the bathymetry divided by the total time. Thus, a location with a relative exposure time of 0% is never exposed and of 100% is always exposed.

Because it was computationally too expensive to perform the calculation for the entire three year period, the exposure time was calculated with both the TRIA and GETM method for one arbitrarily chosen month (April 2009). The results in Figure 3 show large differences between both methods. The TRIA method predicts longer exposure times than GETM of about 2-3% over the watersheds in the eastern part of the Dutch Wadden Sea (yellow and orange), and over 10% shorter exposure times at the edge of the salt marsh just north of the Dutch mainland and over the watersheds in the western part of the Dutch Wadden Sea (deep blue).

Part of the discrepancies between the TRIA and GETM methods was related to small differences at the tidal gauge stations between the observed SLH and the SLH simulated using GETM. The

Root-Mean-Square Error (RMSE) of the simulated as compared with the observed SLH varies between 0.08 and 0.23 m (Figure 4). The RMS Error is defined as:

$$RMSE(i) = \sqrt{\frac{\sum_{t=1}^{N_t}(\hat{y}_t(i) - y_t(i))^2}{N_t}} \quad (1)$$

with $\hat{y}_t(i)$ the SLH observed at the tidal gauge station and $y_t(i)$ the SLH from the simulation with GETM or derived with the TRIA method at the i^{th} grid point for all discrete times t, from 1 to N_t. The RMSEs were small at all locations in the North Sea (nrs. 15, 12, 1, 2 and 8) or close to a wide tidal channel (nrs. 3, 4, 7, 5 and 6). The tidal characteristics were also compared in [15]. This comparison showed good agreement for the semi-diurnal lunar M2 tidal component: the error in the amplitude was 12% at maximum and the phase error less than 20 minutes. Duran-Matute *et al.* (2014) also found that the largest errors occur in the Eastern part of the Dutch Wadden Sea (nrs. 11, 13 and 14; bottom panels in Figure 4). There, tidal gauge stations are mainly located in or near small channels, which may not be properly resolved in the simulation with GETM at a resolution of 200 m. Such errors in the simulated SLH are likely to occur in (shallow) areas in the vicinity of the latter tidal gauge stations and may lead to a significant bias in the estimated exposure time based on these values.

3.3. Comparison of the two methods using simulated SLHs with GETM in TRIA

Even though the GETM model simulates the SLH very well as demonstrated in [15], still small errors in the simulated SLH (as shown in Figure 4) may lead to significant differences in the exposure time. In the comparison between the two methods, TRIA and GETM, we wish to avoid any contribution from differences between observed and simulated SLH at the locations of the tidal gauge stations. Therefore, we now apply the TRIA method using *simulated* SLH at the tide gauges instead of the *observed* SLH. Differences elsewhere in the basin can then no longer be associated with small errors in the GETM simulated SLH at the tidal gauge stations.

This approach may seem rather straightforward, but some of the tidal gauge stations were located in grid-points in the GETM model that were marked as land, such as stations 5 and 9 (see Figure 4), or fall dry (100% exposure) following the post-processing. The latter may occur as the local bathymetry in the GETM model at 200 m resolution was significantly altered due to area-averaging and smoothing. At such locations, the actual local bathymetry is deeper than the averaged and smoothed bathymetry used in the model. The TRIA method cannot be applied to land or "dry" locations, because there the SLH is simply not (always) known. Hence, the grid point nearest to each of the tidal gauge stations, which was submerged throughout the entire simulation period after post-processing, was used instead. The stations Eemshaven, Delfszijl and Nieuwstatenzijl (nrs. 16, 17 and 18 in Figure 1) were outside of the model domain used in [15]. The distance to the nearest continuously submerged gridpoint of the station at Eemshaven was 20 km to the northwest; for the purpose of this exercise, this location was assumed to be a 'tidal gauge station' (red dot nr 16 in the far right in Figure 5).

The RMS Deviation (RMSD) between the simulated (GETM) and the interpolated SLH (TRIA) was calculated for the month of April 2009 from

$$RMSD(i) = \sqrt{\frac{\sum_{t=1}^{N_t}(\hat{y}_t(i) - y_t(i))^2}{N_t}} \qquad (2)$$

The similarity with equation (1) is obvious. However, here, $\hat{y}_t(i)$ was the SLH determined by TRIA and $y_t(i)$ was the SLH from the GETM at the i$^{\text{th}}$ grid point for all discrete times t, from 1 to N_t. Note that in both methods, the SLH was set to the local depth of the bathymetry when exposed ('dry'). This ensures that the difference between the methods becomes zero when they both predict that a location falls dry.

Figure 5 shows that RMSDs are small in deeper areas, which are predominantly in the western part of the Dutch Wadden Sea, e.g. in triangles (4,5,10), (6,7,10) as well as in the tidal channels connecting the inner parts of the Wadden Sea to the inlets. RMSDs are much larger in some areas of the North Sea, resulting from extrapolation of the tidal gauges stations; these areas, however, are never exposed and therefor irrelevant for this study. In these deep parts, the tidal wave approximately behaves linearly and thus a linear interpolation, such as TRIA, works well. The largest RMS deviations occur in the Balgzand area (south of the line connecting station 3 and 5), on the tidal watersheds south of Vlieland (south of station 6) and in the eastern part of the Dutch Wadden Sea, where the local bathymetry becomes increasingly shallow. On these watersheds and the tidal flat, the TRIA method leads to a lower SLH than the ones simulated with GETM (see Figure 5). Two possible causes can be envisioned. First of all, watersheds are located where the tidal waves entering from two neighboring inlets meet, leading to a setup locally over the watershed. Secondly, if a phase difference was present between the three points that form the triangle in the TRIA method, this leads to an artificial reduction of the amplitude of the SLH. This occurs if points within a triangle were placed on either side of a tidal watershed, such as triangles numbered (4,6,10), (7,10,11), (10,11,13) and especially (13,14,16) & (14,15,16). To accommodate these phase differences in the triangulation of Intertides [11], Rappoldt first synchronized the signals according to the average of the lunitidal interval for high and low water or the phase of M2 tide before interpolation. In TRIA, however, we did not apply this ad-hoc synchronization.

Besides the maximum SLH, other differences can be observed between the SLH estimated with the GETM and the TRIA method (Figure 6). During spring tides (Figure 6a), the GETM method suggests that the tidal watershed is never exposed, whereas the TRIA method indicates exposure of about one third of the time. During neap tide (Figure 6b), the GETM method also shows some periods of exposure, but less than the TRIA method. Moreover, a time-lag exists between the time-series, with GETM lagging TRIA with about an hour. This time-lag does not affect the relative exposure; only the exact timing of the exposure is different by about an hour. Finally, the SLH derived from the GETM simulation shows a much stronger asymmetry between the rising and the falling tides that the SLH derived with the TRIA method. The stronger asymmetry in the GETM simulation is not just related to the way drying is modelled, because the asymmetric part is not limited to periods when the local water depth is less than the critical depth of 0.26 m (dashed line). Hence, the largest differences between the GETM simulation and the TRIA method occur during the falling phase of the tide and especially when the water height is very small and approaching zero.

4. OPTIMIZATION BY ADDING ARTIFICIAL TIDAL GAUGES

From the analysis above, it can clearly be deduced that the TRIA method shows strong deviations (up to more than 60 cm in the eastern Wadden Sea) from the GETM model simulation at the watersheds. Nonetheless, the method is appealing in principle because it uses *in-situ* observations at the tidal gauge stations, which have a high accuracy and high temporal resolution. Hence, we take it one step further and investigate what the effect would be of placing additional tidal gauge stations in the Wadden Sea to improve the results with the TRIA method with respect to the GETM simulation. Two questions were addressed: (i) where should the tidal gauge station(s) be placed to get an optimal reduction of the RMS deviation between the TRIA and GETM method and (ii) how many stations need to be placed to reduce the area averaged RMS deviation below a certain value. These questions can be viewed as an optimization problem with the constraint that virtual tidal gauge stations can only be placed at locations that were submerged throughout the simulation time (being April 2009). This constraint optimization problem was solved using a genetic algorithm from MATLAB (www.mathworks.com), which is based on a natural selection process that mimics biological evolution. In successive steps, the algorithm modifies a population of individual solutions by randomly selecting individuals from the current population and uses them as parents to produce children for the next generation. The population then evolves towards the optimal solution after several generations. The starting population consists of all locations that are submerged throughout the month of April 2009 (except for the corners of the triangle), being 3815 individuals.

Figure 7 shows the distribution of the RMS deviation for the triangle formed by the stations Harlingen (number 10 in the South), West-Terschelling (number 7 in the North-West) and Nes (number 11 in the North-East). Hence, it is a zoom of the 'central' triangle in Figure 5. The largest RMS deviations were again found at the tidal watersheds.

The mean RMS Deviation (RMSD) was 0.14 m and was defined as:

$$\overline{RMSD} = \sum_{i=1}^{M} \frac{RMSE(i)}{M-P}, \qquad (3)$$

where M is total number of grid points in the domain and P the total number of tidal gauge stations, e.g. 3 (Harlingen, West-Terschelling and Nes) plus the virtual gauge stations, since P is small compared to M, it was neglected. For this particular triangle, we seek the optimal location for the virtual tidal gauge stations. As a first approach, the additional tidal gauge station was placed at the location where the error was maximum, which was (x, y) = (167, 593) km; this led to a reduction of the mean RMS deviation from 0.14 m to 0.12 m (-19%). The optimal location for placing a tidal gauge, however, was further to the Southwest of this location at (x, y) = (161,584) km and led to a mean RMS deviation of 0.11 m (i.e. 20% less than the difference within a situation without this additional station).

Adding two tidal gauge stations at their optimal location simultaneously would result in a mean RMS deviation of 0.10 m (-29%). It must be noted that neither of the locations at (x, y) = (156, 598) and (x, y) = (167, 593) km of these two virtual tidal gauges was anywhere near the optimal location in the case if only one extra tidal gauge station was added. An almost linear decline exists between the mean RMS and the number of stations added simultaneously (Figure 8). Halving the RMS deviation between TRIA and GETM requires 6 additional stations in the triangle formed by Harlingen (10), West-Terschelling (7) and Nes (11) in a configuration as shown in Figure 7e. Optimal locations for additional stations to reduce mean RMS deviation depend on the number of stations and cannot be directly deduced from spatial patterns in RMS deviations. However, it should be noted that the optimal location of the virtual stations is such that the edges of the triangles are aligned with the channels (Figure 7f). This makes sense, as the SLH would behave almost linearly in these deep channels and therefore best captured by the TRIA method in this configuration. It can be concluded that a linear interpolation between sea level heights at tidal gauges as applied by the TRIA method in principle can provide similar results as the GETM method by adding tidal gauge stations in the Wadden Sea.

5. THE HYBRID METHOD

Variations in Sea Level Height (SLH) in the Wadden Sea are the result of astronomical and shallow-water tides as well as wind-driven set-ups or set-downs. Apart from long-period variations (such as the 18.6 nodal cycle), the tidal characteristics, i.e. amplitude and phase of each constituent, are fairly constant from year-to-year. In contrast, the wind effects are not predictable on those time scales. Hence, one can expect that a model from 2009-2011, say, also applies to other years as far as the tides are concerned, but of course not for the wind-related variations. Here, we propose an approach to estimate exposure times in which the two methods discussed so far were combined to make use of their advantages without suffering from their shortcomings, the so-called HYBRID model.

Using the simulation with the GETM model, a great number of tidal gauges was added at which the tide can be predicted. The wind set-ups and set-downs (including storm surges, generated further away on the North Sea) were extracted from the *in-situ* observations of the SLH at the tidal gauges. It seems plausible that the interpolation of the wind set-ups and set-downs between the tidal gauges must produce a fairly reliable result since these are large-scale phenomena, with spatial and temporal patterns of the size of the Dutch Wadden Sea [25]. Finally, adding the interpolated set-up/set-down to the tidal predicted signal leads to an estimate of the SLH at each point in the domain. One caveat is that the wind-driven and the astronomical components of SLH are not completely independent from each other since the propagation speed of the tide depends on the water depth and thus on the set-up. Although, in principle, these two SLH components cannot be simply added up, we have ignored this in this first exploration.

5.1. Application of the HYBRID method to the Balgzand tidal flat area

We applied a Least Squares Harmonic Analysis (LSHA) using the T_tide [19] to the three-year simulation of the post-processed SLH in the Balgzand area. From the results of the LSHA, a tidal prediction can be determined of the SLH at any moment in time as well as its long-term mean value, according to:

$$SLH(t) = SLH_0 + \sum_{i=1}^{140} A_i \cos(\omega_i t - \theta_i) + \varepsilon(t) = SLH_0 + TP(t) + \varepsilon(t) \qquad (4)$$

Where $SLH(t)$ was the original time-series of the post-processed Sea Level Height, SLH_0 the long-term mean sea level height and $\varepsilon(t)$ the sea level variations unrelated to the tides (e.g. setup or setdown); the summation represents the tidal prediction $TP(t)$, in which A_i, ω_i and θ_i are amplitude, frequency and phase of the ith tidal component. In 87% of the locations on the Balgzand, the tidal prediction (with 146 constituents) explains more than 80% of the variability and at the remaining locations it explains at least 73%. Note that, the harmonic analysis was applied to the post-processed SLH data, including the interpolated SLHs that turned out to be below the local bathymetry. This ensures that no gaps are present in the time-series data, even during times when a certain location is sometimes exposed within the 3-year time-series. This choice was made, because gaps during low tide would lead to a biased SLH_0, e.g. too high, if SLHs during low water are absent from the time-series as a result of being exposed.

The long-term mean sea level height, SLH_0, in Figure 9 shows relatively high values of nearly 0.25 m above NAP in the shallower part of the area, e.g. the water seems to be pushed onto the tidal flat. In the deeper parts, e.g. in the Marsdiep tidal inlet, the Texelstroom tidal channel and parts of the Malzwin tidal channel, the long-term mean SLH_0 was close to zero. There, the non-linear effects that may cause a long-term mean SLH_0 were negligible.

Now, the wind setup was calculated from SLH observations at the tidal gauge stations of Den Helder (3), Den Oever (5) and Oudeschild (4) (Figure 1), after extracting the tidal signal by harmonic analysis. The setup from the observations at the tidal gauge stations was subsequently interpolated to all locations on the Balgzand area using the TRIA method (SLH_{TRIA}; m). The RMS difference between the two setups, e.g. the one derived from the harmonic analysis, $\varepsilon(t)$, and the one derived using TRIA, SLH_{TRIA}, is shown in Figure 10. In the region that was submerged continuously (in the Northern and Eastern part of the figure), the RMS deviation was very small, e.g. < 0.06 m. Furthermore, the maximum RMS deviation on the shallow tidal flat, being 0.15 m, was smaller than the one between the SLH themselves, which was > 0.4 m for the same area (see Figure 5). The largest errors were observed on the Balgzand tidal flat, where the pattern of the long-term mean SLH_0 seems to be reflected (compare Figure 9 and Figure 10). Especially there, an impact of an error in the estimated SLH on the exposure time can be expected.

During the month of June 2012, pressure sensors were placed at several locations on the Balgzand tidal flat (Figure 11), of which the data (SLH_{OBS}; m) will be used for further validation of the methods. Pressure sensor P10 was located in the triangle formed by the tidal gauge stations, Den Helder (DH, 3), Den Oever (DO, 5) and Oudeschild (OS, 4), whereas P03, P05 and P08 were slightly south of the line between Den Oever and Oudeschild (see also Table 1). They were placed as part of a study to the foraging behaviour of Oystercatchers [20] and used to obtain more accurate water level estimation in the Balgzand area with the triangulation method [11] by locally increasing the number of independent SLH observations in the network.

The comparison between the observed SLHs at the pressure sensors and the interpolated values using the TRIA method are shown in Figure 12. Note that the grey points represent data for which the pressure gauges indicate that the SLH was above the seabed (i.e. submerged), whereas the TRIA method suggests a SLH below the bed (i.e. emerged). Two linear correlations were calculated, i.e. one in which the emerged points were taken into account (black) and one in which they were excluded (red) (Figure 12). The comparison shows a good correlation for P10 (R^2=0.99, when emerged points were excluded), which is not surprising as it was located inside the triangle at a reasonably deep location, D = -0.65 m, and close to the Malzwin tidal channel (distance ~ 180 m, Table 1), where non-linear effects were expected to be relatively small. The method also works fine for the location of P03, although with a larger spread around the fit, leading to a somewhat smaller R^2 (0.93). At locations P05 and especially at P08, which are both located above Amsterdam Ordnance Datum, the SLH was significantly underestimated by 0.10 and 0.20 m (black), respectively. Note that this primarily is related to taking the grey points into account in the linear fit (black); these cause a bias towards underestimating the SLH in the TRIA method. At stations P05 and P08, the observed SLHs are higher than obtained through the TRIA method. This may be related to the phase difference between Den Helder and Den Oever. However, observed high water levels at P08 were (with some exceptions) higher than either level at the Den Helder and the Den Oever tidal gauge station within the same tidal phase (Figure 13). Therefore, even if a phase adaption were implemented as proposed in [11], the (maximum) SLHs at P08 would not be reproduced satisfactorily. At location P08, the shallowest of the four (D = -0.21 m), the tidal signal contains a local time-independent setup as was already indicated in Figure 9, leading to an offset between the maximum SLHs at the Den Helder and Den Oever tidal gauge stations, on the one hand, and the maximum SLH at location P08, on the other.

Figure 14 shows the comparison between the observations and the combined HYBRID method. For P03, the fit was not as good as with the TRIA method and the spread at P10 was marginally larger, which could be related to the difference in observed and modelled depth, locally (Table 1). At P08, some improvement can be observed, but the most significant improvement was found for location P05, where both the spread was reduced and the fit moved closer to the one-to-one line. Pressure sensors P05 and P08 were located relatively high on the intertidal flat (Table 1) and fall dry a significant amount of the time, reducing the amount of observations for making a fit. Besides that, they were located next to a small tidal gully, south of the edge of the triangle between Den Oever and Den Helder. Both the significant distance from this line and the shallowness, which influences the progressing tidal wave significantly (frictional effects) due to the non-linear interaction between the different tidal components, apparently cause the linear triangulation method (TRIA) to be less successful at these locations.

In summary, the HYBRID method shows improvement at some locations in estimating the local SLH, but not at all locations on the Balgzand tidal flats. However, it is not clear whether the estimate of the exposure time also improves. At all locations, except P03, the estimate of the exposure time with the combined method (HYBRID) was closer to that of the observations than that using the triangulation method (TRIA, Table 1). The reason why the combined method works so poorly at station P03 may be related to the coarse resolution bathymetry used in GETM, leading to a modelled bathymetry level of D = 0.88 m at the nearest grid point (Table 1). Besides that, errors in the determination of the position and height (using GPS) of the pressure sensor may cause significant differences in the exposure time, if the “true” location was significantly different.

Note that the pressure sensors were placed in and near one of the smallest triangles which covered the Wadden Sea in the triangulation method and that no watershed was crossed by this triangle. Hence, the triangulation method (TRIA) can be expected to have the most successful results there compared with other locations, such as in the central part of the Dutch Wadden Sea, where triangles cross one or more watersheds. Thus, showing an improvement with the combined method (HYBRID) for three out of four of these locations, suggest that this method might even be more promising in other parts of the Wadden Sea, which will be explored in the next section.

5.2. Application of the HYBRID method to the Dutch Wadden Sea

Similar in-situ observations as those on the Balgzand area are lacking elsewhere in the Wadden Sea, except of course for the measurements at the tidal gauge stations. Therefore, in the following experiment, data at one of these tidal gauge stations was discarded in the triangulation method and reserved as ‘a record for verification’. In this experiment, we also include three stations in the North Sea (Petten, 1; Texel Noordzee, 2 and Terschelling Noordzee, 8). The tidal gauge stations marked yellow in Figure 15 (top) have one-by-one been left out from the triangulation method and were used for verification (as an example station 14 has been left out in the bottom panel of Figure 15). Only these stations were chosen, because they were located within the outer boundary formed by the triangles. Moreover, instead of the triangles defined in [11] (as in Figure 1), a Delaunay triangulation was applied. In mathematics and computational geometry, a Delaunay triangulation for a set of points in a plane was such that no point was inside the circumcircle of any triangle. Delaunay triangulations maximize the minimum angle of all the angles of the triangles in the triangulation; they tend to avoid skinny triangles [21].

The result for each of the tidal stations that was left out is given in Table 2. The RMS deviation with the simulations (GETM) was sometimes larger than the ones derived with the triangulation method (TRIA), particularly at Schiermonnikoog. Here the local bathymetry strongly deviates from the smoothed version used in the GETM simulation and the location was also quite close to the open boundary. Overall, both methods have a similar error, as is evident from the equal mean value for the nine stations. However, the HYBRID method clearly performs much better than the previous methods, which was reflected in RMS deviation that was reduced by a factor three. Moreover, the maximum error was only 0.07 m at maximum and was found at the location called Nes (11). By using this station for verification and thus leaving it out from the triangulation, introduced a significant 'gap' in the web created by the triangles covering more than one tidal watershed.

6. SUMMARY AND DISCUSSION

In this study we have compared three methods to determine the exposure times of the intertidal flats in the Dutch Wadden Sea: (i) a triangulation method (TRIA) that interpolates observed Sea Level Height records from tidal gauges, (ii) a calculation based on a simulation with a hydrodynamic model (GETM), and (iii) a HYBRID method combining the previous two. The triangulation method has the advantage of being based on truly observed records from the tidal gauges, but the disadvantage of interpolating between stations that lie across watersheds in two different tidal basins, impairing the representation of tidal phase propagation. The GETM model simulation has the advantage of dynamically including differences in the phase of the tide, but still has problems inherent to the model. This includes the lack of resolution of the finer bathymetric features and the "flooding and drying"-algorithm, in which water level never really reaches zero in the model simulation, but in which the advective terms were effectively switched off below a certain threshold value. The treatment of flooding and drying in GETM may lead to artificially high sea levels near tidal watersheds even though wetting fronts appear to be well-represented in models that use this type of method [12, 22]. Compared to the outcomes of the GETM method, the TRIA method can underestimate exposure times by more than 10%, in particular near watersheds in the western part of the Dutch Wadden Sea.

The virtual experiment in a subsection of the Wadden Sea demonstrates that a large number of additional tidal gauges is needed to reduce the deviation between the TRIA and GETM methods. This finding is supported by the comparison between the measurements on the Balgzand using pressure gauges and the TRIA method, even though, one of the pressure gauges displayed higher maximum sea level heights than observations at the tidal gauge stations that were used in the TRIA method during the same tidal phase.

As an alternative, we have proposed a third method (referred to as HYBRID) by combining the two first methods to capture the best of both worlds. First, we extract from the model the signal of the tide by means of a tidal harmonic analysis, at every gridpoint of the model similar as was done in the Balgzand area. Thus, we take into account the subtleties of tidal phase propagation through the channels in the different basins. Secondly, we calculate the wind-driven contribution to sea level from tide gauge records by applying a tidal harmonic analysis and extracting the residual. These meteorologically induced variations were then interpolated for every grid cell by means of triangulation. The combination of the tidal and wind induced signals, at every gridpoint, then gives the estimate of the SLH.

Subsequently, we compared the performance of these three methods against records of Sea Level Height from pressure sensors on the Balgzand area. There, the HYBRID method performed better than the TRIA method at three out of four locations. The station at which the HYBRID method does not perform well shows a large difference between the observed (-0.2 m) and modelled bathymetry (-0.9 m). This difference can either be caused by errors in the GPS location of the sensor, or the smoothed bathymetry in the GETM model. Expected RMS errors in the modelled SLH are in the order of 0.1 to 0.2 m as is the case with the tidal gauge stations (see Figure 4).

At the Balgzand area, however, the triangle in which the SLH is interpolated is relatively small and no watersheds were crossed. This testing area is therefore not encompassing the full complexity as found at other locations in the Wadden Sea. As an alternative check, we predicted SLH at individual tidal gauge station (one at each time) based on the information from all the others, The result (Table 2) shows very clearly that the combined method HYBRID outperforms the other two methods. In summary: the non-linear tidal behaviour is well-represented in the tidal prediction based on the GETM simulation; the unpredictable part can be accurately determined using the TRIA method based on the *in-situ* observations at the tidal gauge stations and the HYBRID method is computationally efficient. In a future study, a comparison between satellite derived exposure times [23] and the ones derived with the GETM simulations, the TRIA method and the HYBRID method should be performed.

As a final note, we emphasize that benthic biological processes are critically dependent on whether a location is fully emerged or if a pool of water remains during low tide (Figure 16). This implies that a highly accurate and extremely detailed bathymetry is required, e.g. by modelling subgrid-scale bathymetric features [24], to correctly estimate the exposure time at these scales. However, the HYBRID will aid to answer the major (ecological) questions as referred to in the introduction. Once regularly applied (as intended by NIOZ), we will not only be able to hindcast the emersion time but, when taking SLH predictions into account as made available by RWS, even forecast for several days ahead. Such forecasts would enable nature conservation measures, e.g. additional protection of remaining emerged tidal flats as foraging grounds for waders during predicted storm surges. In addition, the HYBRID method could even be applied in other coastal intertidal areas worldwide where accurate information on bathymetry and on SLH from gauges is available and where accurate meteorological data and boundary conditions are available to perform simulations with the GETM model.

7. REFERENCES

[1] de Jonge, V.N.; van Beusekom; J.E.E. (1992) Contribution of resuspended microphytobenthos to total phytoplankton in the Ems estuary and its possible role for grazers. Netherlands Journal of Sea Research, 30, 91–105

[2] Quayle, D.B. (1988) Pacific oyster culture in British Columbia, Can. Tech. Rep. Fish. Aquat. Sci., 218, 1–241

[3] Buschbaum, C.; Saier, B. Growth of the mussel Mytilus edulis L. in the Wadden Sea affected by tidal emergence and barnacle epibionts, Journal of Sea Research, 45 (1), 27-36.

[4] Bayne, B. L.; Hawkins, A. J. S.; Navarro, E. (1988) Feeding and Digestion in Suspension-Feeding Bivalve Molluscs: The Relevance of Physiological Compensations Amer. Zool. 28 (1): 147-159

[5] Brinkman, A.; Dankers, N.; van Stralen, M. (2002) Mussel beds Tidal flats Wave action Sediment composition Habitat suitability map, Helgoland Marine Research 56 (1), 59-75

[6] Walles, B.; Fodrie, F.J.; Nieuwhof, S.; Jewell, O.J.D., Herman, P.M.J.; Ysebaert, T. (2016) Guideline for evaluating performance of oyster habitat restoration should include tidal emersion: reply to Baggett *et al.*, Resoration Ecology, 24 (1), 4-7.

[7] Sanchez-Salazar, M.E.; Griffiths, C.L.; Seed, R. (1987) The interactive roles of predation and tidal elevation in structuring populations of the edible cockle, Cerastoderma edule, Estuarine, Coastal and Shelf Science, 25(2) 245-260

[8] Compton, T.J., Holthuijsen, S., Koolhaas, A., Dekinga, A., ten Horn, J., Smith, J., Galama, Y., Brugge, M., van der Wal, D., van der Meer, J., van der Veer, H.W. & Piersma, T. (2013). Distinctly variable mudscapes: distribution gradients of intertidal macrofauna across the Dutch Wadden Sea. Journal of Sea Research, 82, 103-116.

[9] Kraan, C., van Gils, J. A., Spaans, B., Dekinga, A., Bijleveld, A. I., van Roomen, M., Kleefstra, R. & Piersma, T. 2009. Landscape-scale experiment demonstrates that Wadden Sea intertidal flats are used to capacity by molluscivore migrant shorebirds. Journal of Animal Ecology, 78, 1259-1268.

[10] Nauw, J.; Merckelbach, L.; Ridderinkhof, H. & van Aken, H. (2014) Long-term ferry-based observations of the suspended sediment fluxes through the Marsdiep inlet using acoustic Doppler current profilers Journal of Sea Research, 87, 17 - 29

[11] Rappoldt C.; Roosenschoon, O.R.; van Kraalingen; D.W.G. (2014) Intertides: maps of the intertidal by interpolation of tidal gauge data. EcoCurves Rapport 19, EcoCurves BV, Haren, ISSN 1872-5449.

[12] Duran-Moro, M. Drying and flooding in the Wadden Sea, MSc report NIOZ, 2013.

[13] Elias, E. and Wang, Z. B. (2013) Abiotische gegevens voor monitoring effect bodemdaling, technical report Deltares.

[14] Burchard, H. and Bolding, K. (2002) GETM, a general estuarine transport model. European Commission, Ispra.

[15] Duran-Matute, M.; Gerkema, T.; de Boer, G.J.; Nauw, J.J. and Gräwe, U. (2014) Residual circulation and freshwater transport in the Dutch Wadden Sea: a numerical modelling study, *Ocean Science*, 10, 611-632.

[16] Sha, L.P. (1989) Variation in ebb-delta morphologies along the West and East Frisian Islands, The Netherlands and Germany, Marine Geology, 89, 11-28

[17] Perluka, R.; Wiegmann, E.B.; Jordans, R.W.L. and Swart, L.M.Th. (2006) Opnametechnieken Waddenzee. AGI Rijkswaterstaat, Rapp. Nr. AGI-2006-GPMP-004

[18] Wiegmann, N.R.; Perluka, S.; Oude Elberink, J. and Vogelzang (2005) Vaklodingen: de inwintechniek en hun combinaties. AGI Rijkswaterstaat, Rapp. Nr. AGI-2005-GSMH-012

[19] Pawlowicz, R.; Beardsley, B.; Lentz, S. (2002) Classical tidal harmonic analysis including error estimates in MATLAB using T_TIDE, Computers & Geosciences 28.8, 929-937.

[20] Dokter, A.M.; van Loon, E.E.; Rappoldt, C; Oosterbeek, K.; Baptist, M.J.; Bouten, W.; Ens, B.J. (2017) Balancing food and density-dependence in the spatial distribution of an interference-prone forager, *Oikos*, doi: 10.1111/oik.04139.

[21] Delaunay, B. (1934) "Sur la sphère vide." Izv. Akad. Nauk SSSR, Otdelenie Matematicheskii i Estestvennyka Nauk 7.793-80: 1-2.

[22] Medeiros, S. C.; Hagen, S. C. (2013) Review of wetting and drying algorithms for numerical tidal flow models, Int. J. Numer. Meth. Fluids 71, 473–487

[23] Van Der Wal, D.; Herman, P.M.J. (2007) Regression-based synergy of optical, shortwave infrared and microwave remote sensing for monitoring the grain-size of intertidal sediments." Remote Sensing of Environment 111.1, 89-106.

[24] Sehili, A.; Lang, G.; Lippert, C. (2014) High-resolution subgrid models: background, grid generation, and implementation, Ocean Dynamics, 64.4, 519-535.

[25] M. Duran-Matute, T. Gerkema & M. G. Sassi (2016) Quantifying the residual volume transport through a multiple inlet system in response to wind forcing: The case of the western Dutch Wadden Sea. J. Geophys. Res. 121, 8888-8903.

ACKNOWLEDGEMENTS

This study was performed within the framework of the Wadden Sea Long-Term Ecosystem

Research (WaLTER) project, which was financially supported by the Waddenfonds, provinces of Fryslân and Noord-Holland. We acknowledge Bruno Ens (Sovon) for supplying us with the pressure data of Balgzand tidal flats. We would also like to thank the anonymous reviewers; their comments and suggestions led to a significant improvement of the paper.

LIST OF FIGURES

Figure 1: Locations of the tidal gauge stations in the Dutch part of the Wadden Sea and the adjacent coastal zone of the North Sea. Numbers correspond to the following stations from west to east: 1) Petten Zuid; 2) Texel Noordzee; 3) Den Helder; 4) Oudeschild; 5) Den Oever; 6) Vlieland haven; 7) West-Terschelling; 8) Terschelling Noordzee 9) Kornwerderzand; 10) Harlingen; 11) Nes; 12) Wierumergronden; 13) Lauwersoog; 14) Schiermonnikoog; 15) Huibertgat; 16) Eemshaven; 17) Delfszijl; 18) Nieuwstatenzijl. Definition of the triangles as used in the triangulation method (TRIA) following [11]. The colors in the background indicate the bathymetry derived from cycle 5 [13].

Figure 2: Top: Difference between the vaklodingen taken for the years closest in time (either in the past or the future) to the years 2009-2011 of the simulation (as in [15]) and the cycle 5 data; Bottom: same as top, but for cycle5 data with shifted grid (i.e. bathymetry was shifted 10 m to the west and 10 m to the south).

Figure 3: Difference between relative exposure times (%exposureTRIA-%exposureGETM) as predicted by triangular (TRIA) and the General Estuarine Tidal Model (GETM) method as estimated for April 2009.

Figure 4: Smoothed bathymetry used in the GETM simulation (colors) and cycle 5 bathymetry (contours; every 2.5 m in general and 5 m for stations 3 & 4). The title of each panel indicates the station number (right) as given in Figure 1 and the RMS error (left, in m) between the observed SLH and simulated SLH with GETM for the period 2009-2011.

Figure 5: Distribution of the RMS deviation in Sea Level Height (SLH; m) between the simulation with GETM and the TRIA method (i.e. The root of the sum of $(SLH_{TRIA}-SLH_{GETM})^2$ per grid point divided by the number of discrete times) applied to the continuously submerged grid points nearest to the tidal gauge stations (indicated with red dots) in April 2009.

Figure 6: SLH estimated with the TRIA (red) and the GETM (blue) method at location (x,y)=(165,595) km, e.g. on the watershed of Terschelling. The dashed line indicates the critical water depth of 0.26 m. Panel a) shows the SLH curves at spring tide and panel b) at neap tide.

Figure 7: a) RMS deviation in the triangle formed by Harlingen (10), West-Terschelling (7) and Nes (11) for April 2009. b) Same as in a) but with an additional tidal gauge located at (x, y) = (162,586) km, where the RMS deviation was maximal in panel a). c) Same as in a) but with an additional tidal gauge located in the most optimal location at (x, y) = (160,584)

km, e.g. giving the smallest mean RMS deviation. d) Same as in a) but with two tidal gauge stations added simultaneously leading to the smallest RMS deviation, being at (x, y) = (165, 591) and (x, y) = (156, 599) km. Panel e) shows the optimal locations of the additional tidal gauges stations, if 6 ones are allowed and panel f) shows the same configuration of tidal gauges stations superposed on the local bathymetry,

Figure 8: Mean RMS deviation determined for different amounts of additional stations placed simultaneously in the triangle formed by Harlingen (10), West-Terschelling (7) and Nes (11). The mean RMS deviation without any additional station was 0.14 m and reduces by one half after adding 6 tidal gauge stations.

Figure 9: The long-term mean Sea Level Height (SLH_0; m) as derived from the Least Squares Harmonic Analysis applied to the simulated SLHs with GETM in the Balgzand area for three years (2009-2011).

Figure 10: Spatial distribution of the RMS deviation of the wind-driven setup (m) as derived from a Least Squares Harmonic Analysis on the simulated SLHs with the GETM method (SLH_{LSHA}; m) and based on the SLHs observations at the tidal gauge stations with the triangular method (SLH_{TRIA}; m) for three years (2009-2011).

Figure 11: Locations of the pressure sensors, P03, P05, P08, P10 and the locations of the nearest tidal gauge stations Den Helder (DH), Den Oever (DO) and Oudeschild (OS) projected on a map of the “cycle 5” bathymetry.

Figure 12: Interpolated SLH using the TRIA method versus the observations of SLH at the pressure sensors. Dashed line is the one to one line and the drawn line was the best fit. Grey dots indicate that the estimated SLH using TRIA was below the local height of the bathymetry (hence, dry), but observations of SLH were present, e.g. the location in fact was wet. These emerged points were not taken into account in the linear fit marked red.

Figure 13: Mean of the maximum Sea Level Height observed at the tidal gauge station in Den Helder and Den Oever (max $SLH_{DO,DH}$; m) against the maximum SLH observed at the pressure gauges (max SLH_{OBS}; m) for each tide in June 2012. The errorbar gives the range between the value observed at the Den Helder and Den Oever tidal gauge station. Dashed is the one-to-one line and drawn was the best linear fit.

Figure 14: Same as Figure 12, but with the SLH derived from the HYBRID method on the vertical axis, e.g. a combination of the wind-driven setup using the triangulation method added to the tidal prediction derived from a LSHA on the simulation with GETM for the location of the pressure sensors (SLH_{HYBRID}; m).

Figure 15: Top: Delaunay triangulation at locations of tidal gauge stations in and near to the Wadden Sea. Stations marked with yellow dots were removed one at the time from the triangulation and subsequently used for verification of predictions based on all other stations. Bottom: Example of Delaunay triangulation where the sea level heights at one station, e.g. “Schiermonnikoog” (14; yellow dot), was used for verification and therefore left out from the triangulation.

LIST OF TABLES

Table(s)

	P03	P05	P08	P10
Longitude	4˚ 51.38’	4˚ 48.35’	4˚ 38.71’	4˚ 50.73’
Latitude	52˚ 56.60’	52˚ 56.73’	52˚ 55.33’	52˚ 58.11’
RTK-dGPS Observed bathymetry (m NAP)	-0.21	0.28	0.46	-0.65
Cycle 5 bathymetry (m NAP)	-0.50	0.12	0.22	-1.11
Modelled bathymetry GETM (m NAP)	-0.88	-0.04	+0.14	-2.33
Distance to gully (m)	535±261	398±6	670±90	182±24
Mean Height bathymetry cycle5 (m NAP)	-0.95±1.08	-0.63±1.85	-0.28±1.34	-2.55±2.22
Observations	0.37	0.57	0.66	0.16
TRIA	0.37	0.61	0.79	0.14
HYBRID	0.21	0.56	0.75	0.15

Table(s)

Name	**Nr. (Fig. 1)**	**SLH_{GETM}**	**SLH_{TRIA}**	**SLH_{HYBRID}**
Den Helder	3	0.09	0.05	0.03
Harlingen	10	0.15	0.21	0.06
Kornwerderzand	9	0.13	0.11	0.05
Nes	11	0.18	0.24	0.07
Oudeschild	4	0.09	0.12	0.04
Schiermonnikoog	14	0.23	0.14	0.04
Vlieland Haven	6	0.13	0.08	0.02
West Terschelling	7	0.11	0.18	0.04
Wierumergronden	12	0.08	0.06	0.03
Mean RMS deviation		**0.13**	**0.13**	**0.04**

Figure(s)
Click here to download high resolution image

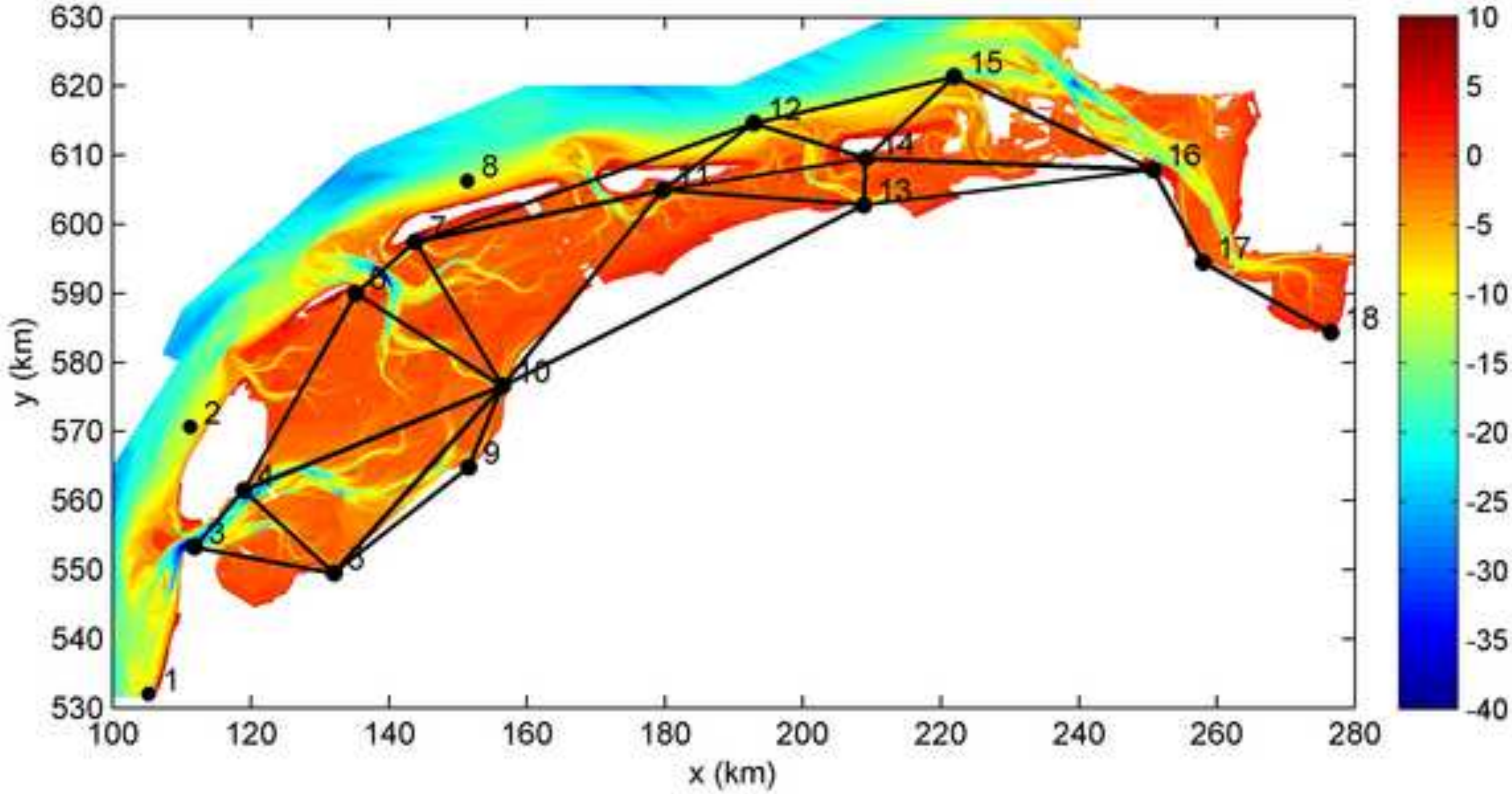

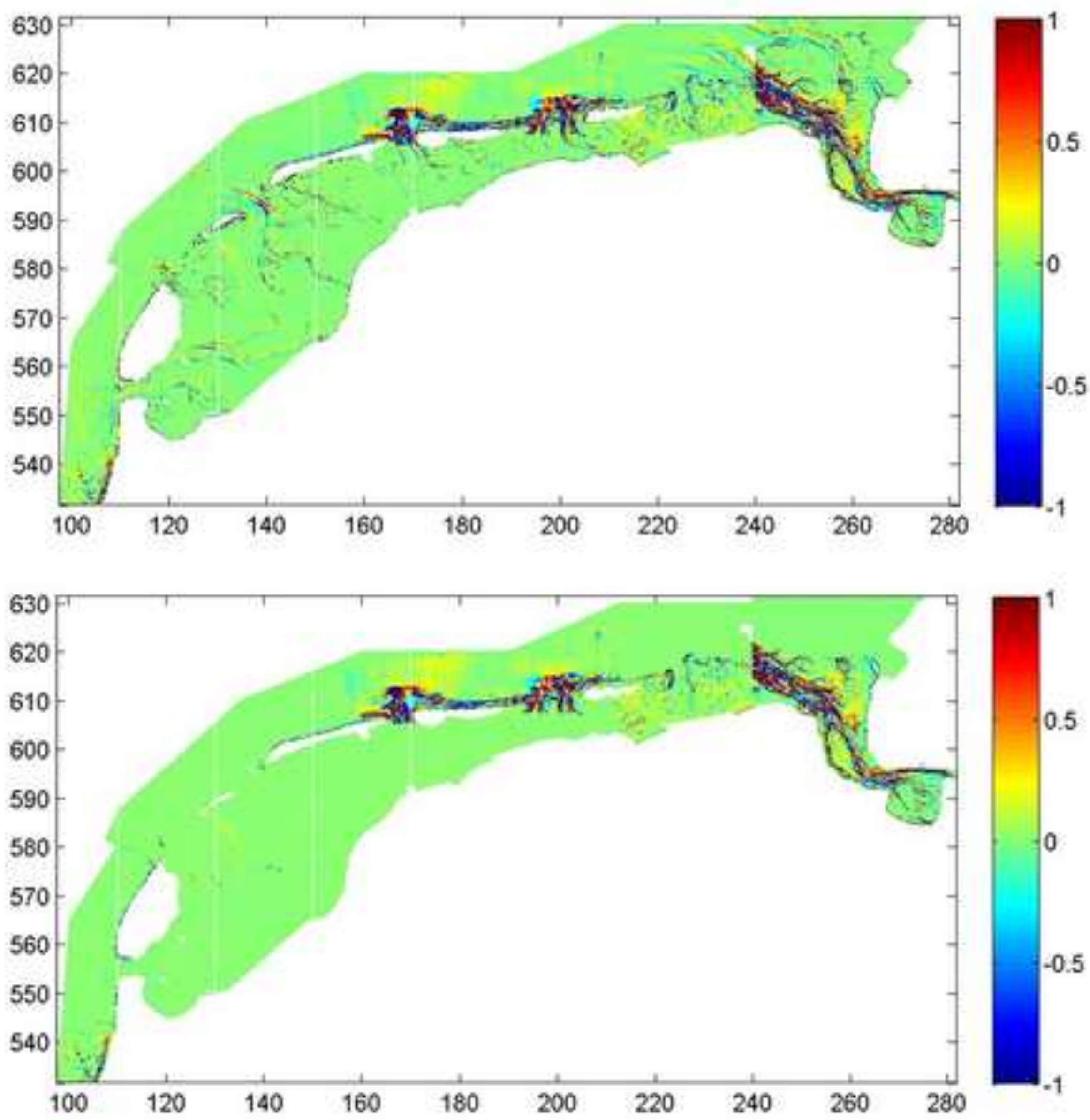
630
620
610
600
590
580
570
560
550
540
100
120
140
160
180
200
220
240
260
280
1
0.5
0
-0.5
-1
630
620
610
600
590
580
570
560
550
540
100
120
140
160
180
200
220
240
260
280
1
0.5
0
-0.5
-1

Figure(s)
Click here to download high resolution image

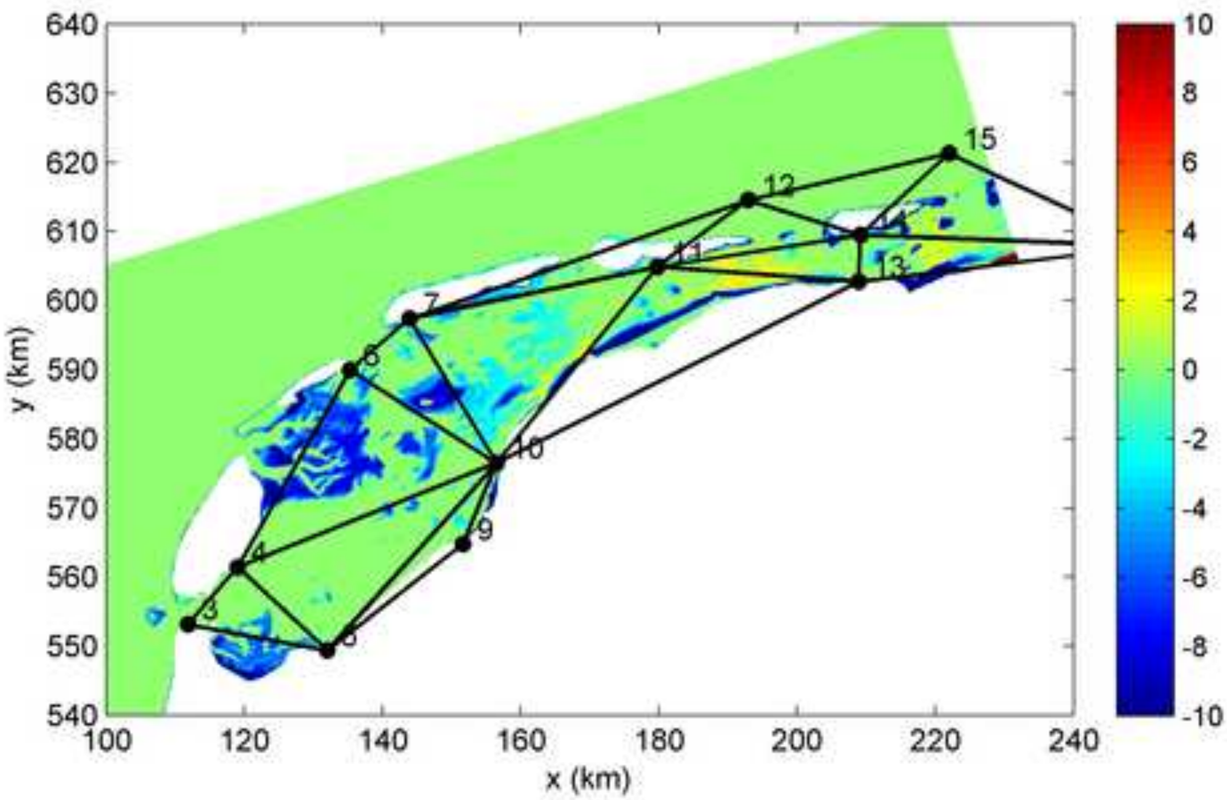

Figure(s)

Click here to download high resolution image

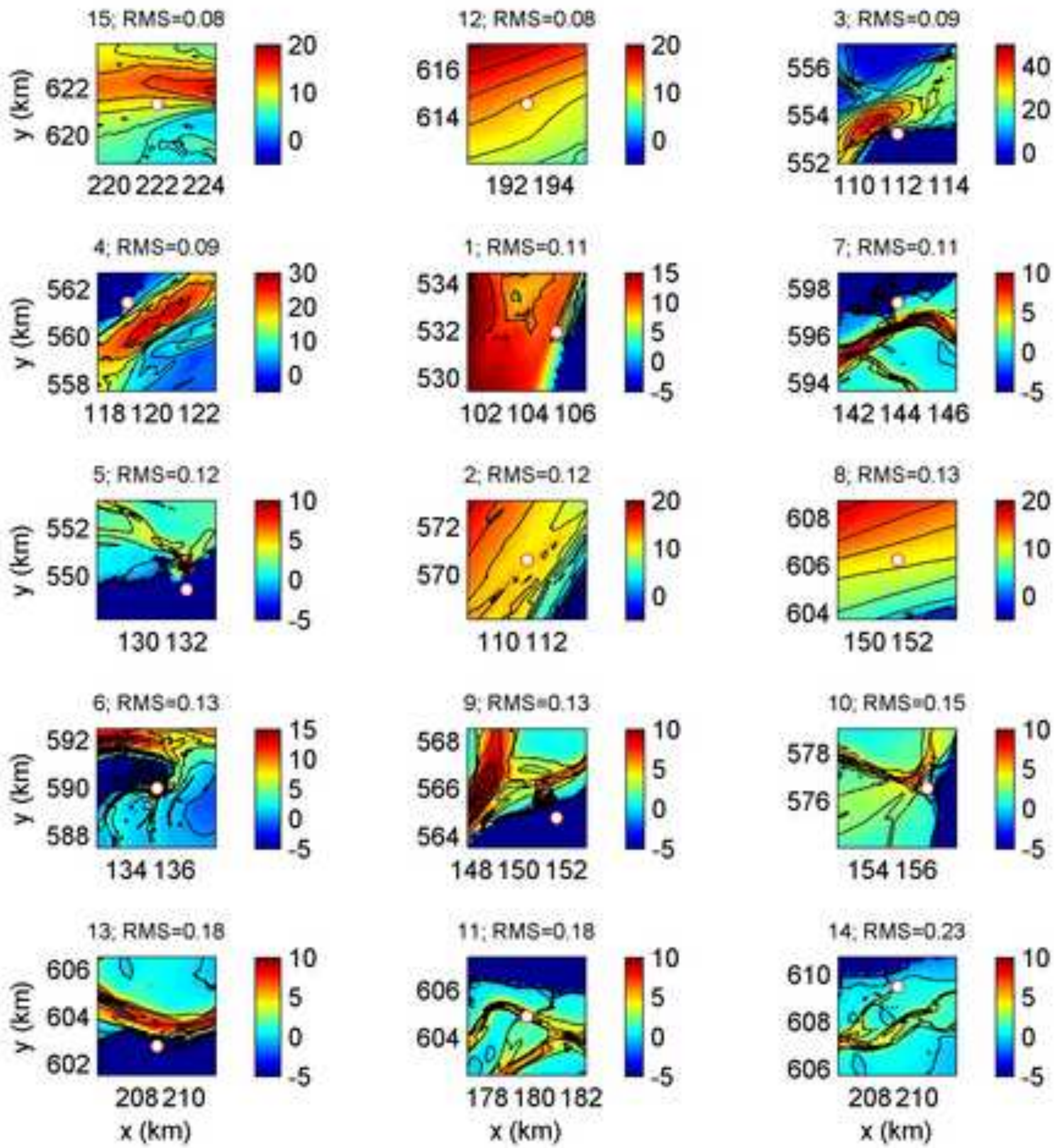

Figure(s)
Click here to download high resolution image

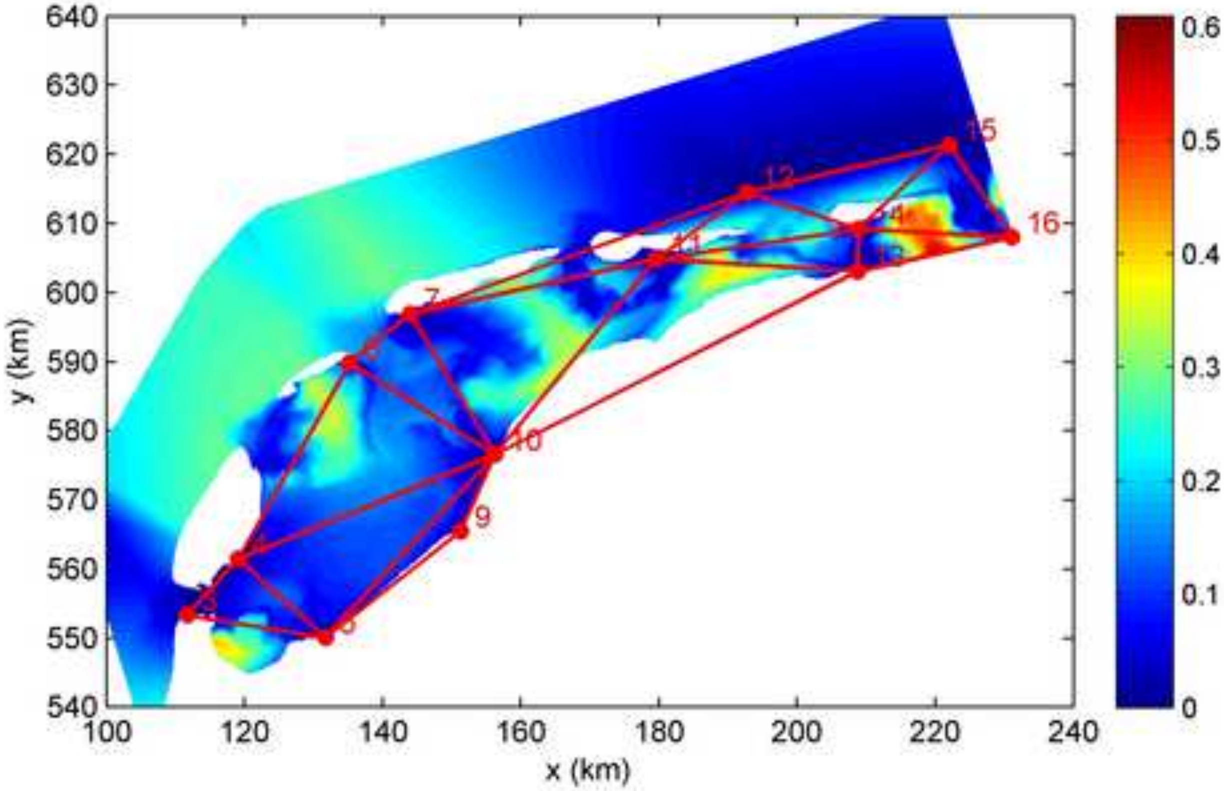

Figure(s)
Click here to download high resolution image

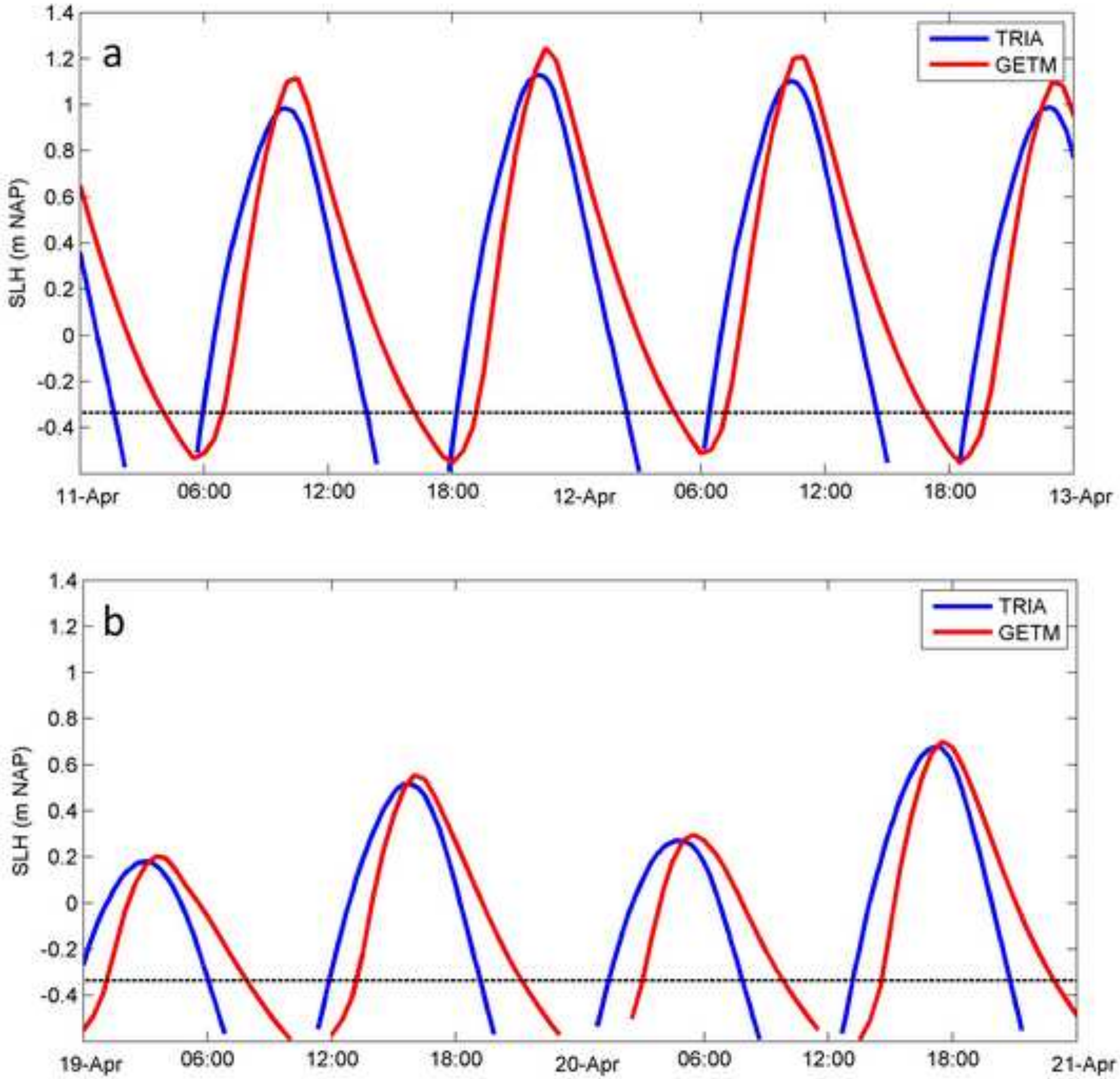

Figure(s)
Click here to download high resolution image

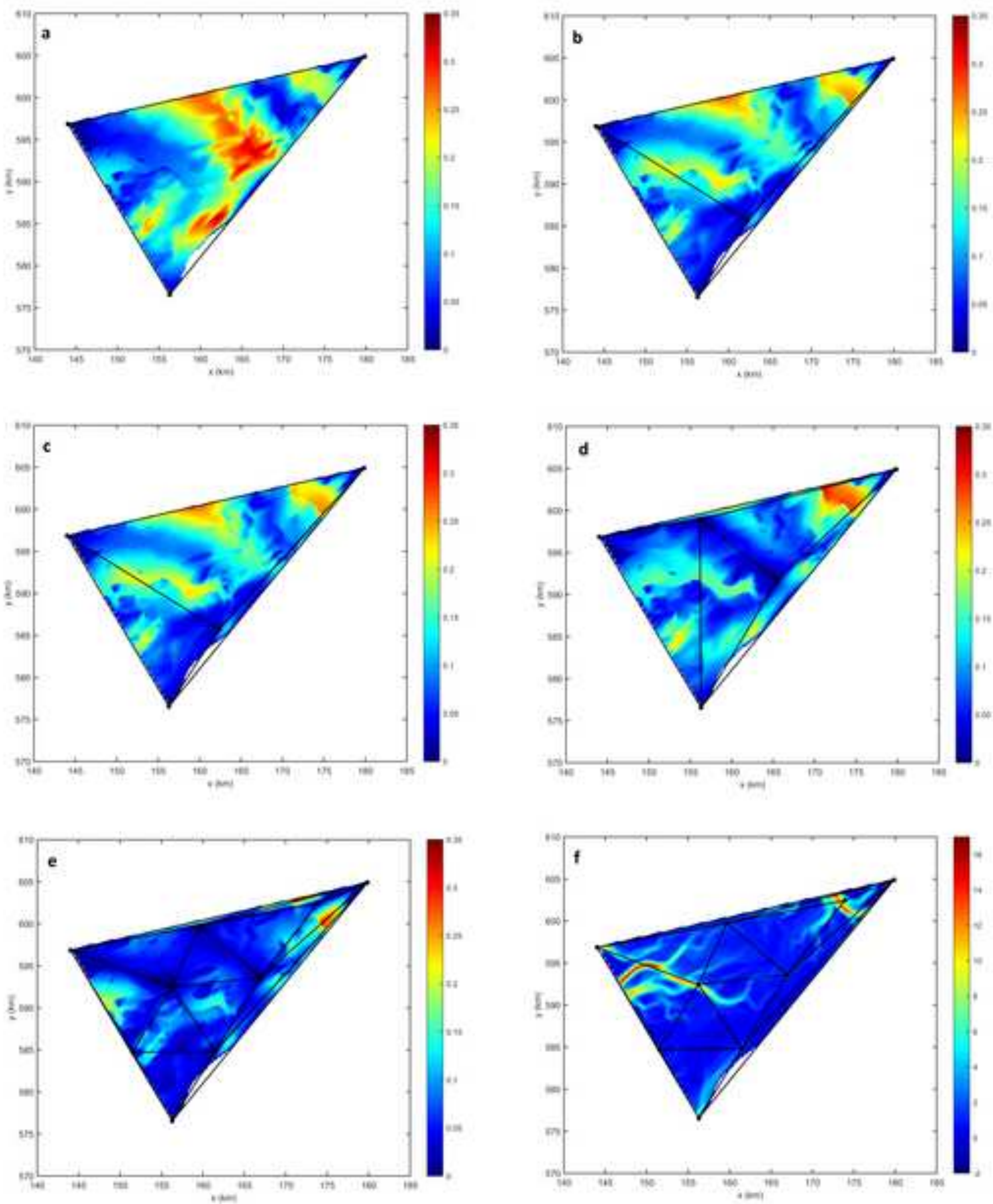

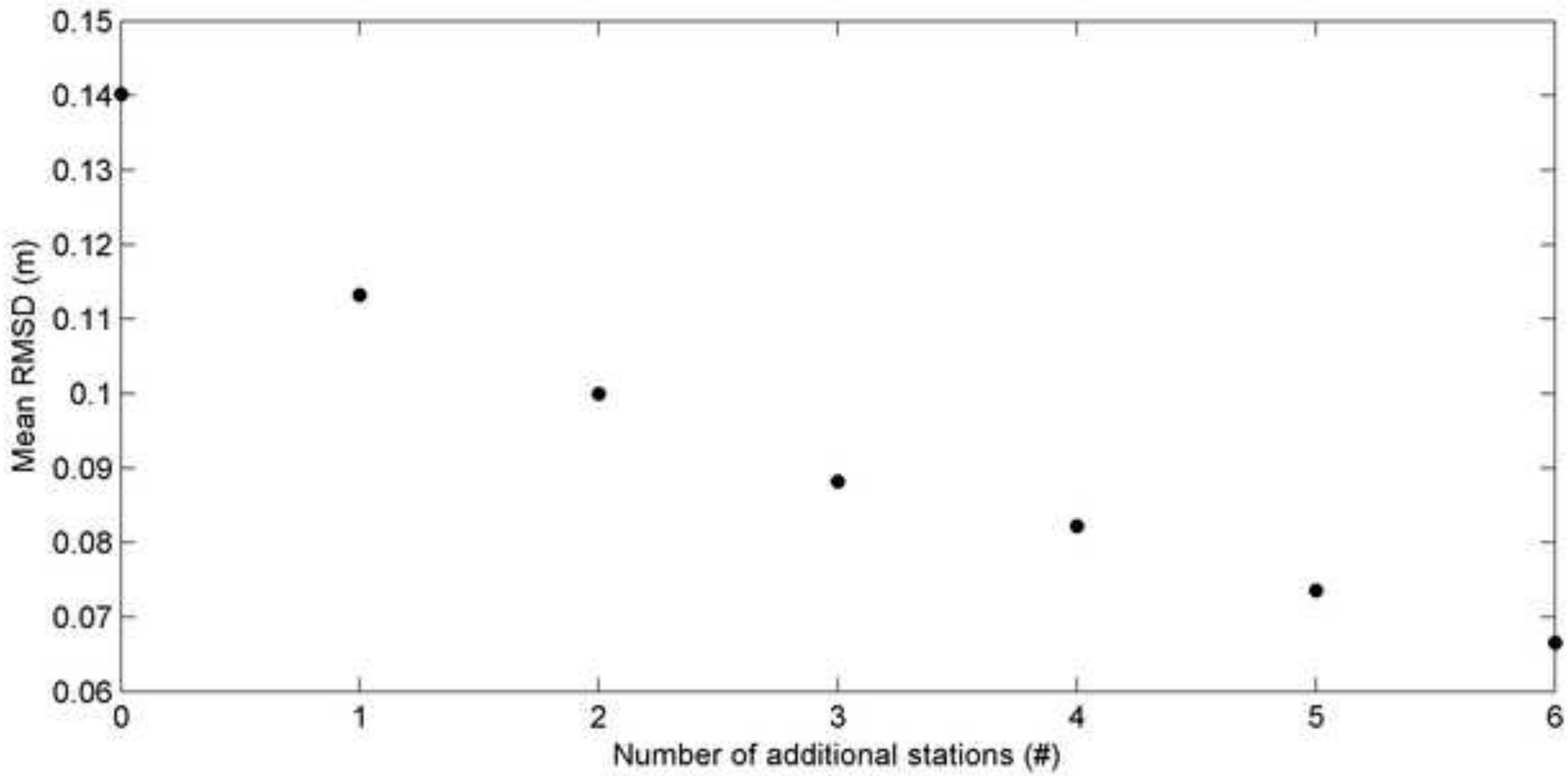
0.15
0.14
0.13
0.12
0.11
0.1
0.09
0.08
0.07
0.06
Mean RMSD (m)
0
1
2
3
4
5
6
Number of additional stations (#)

Figure(s)
Click here to download high resolution image

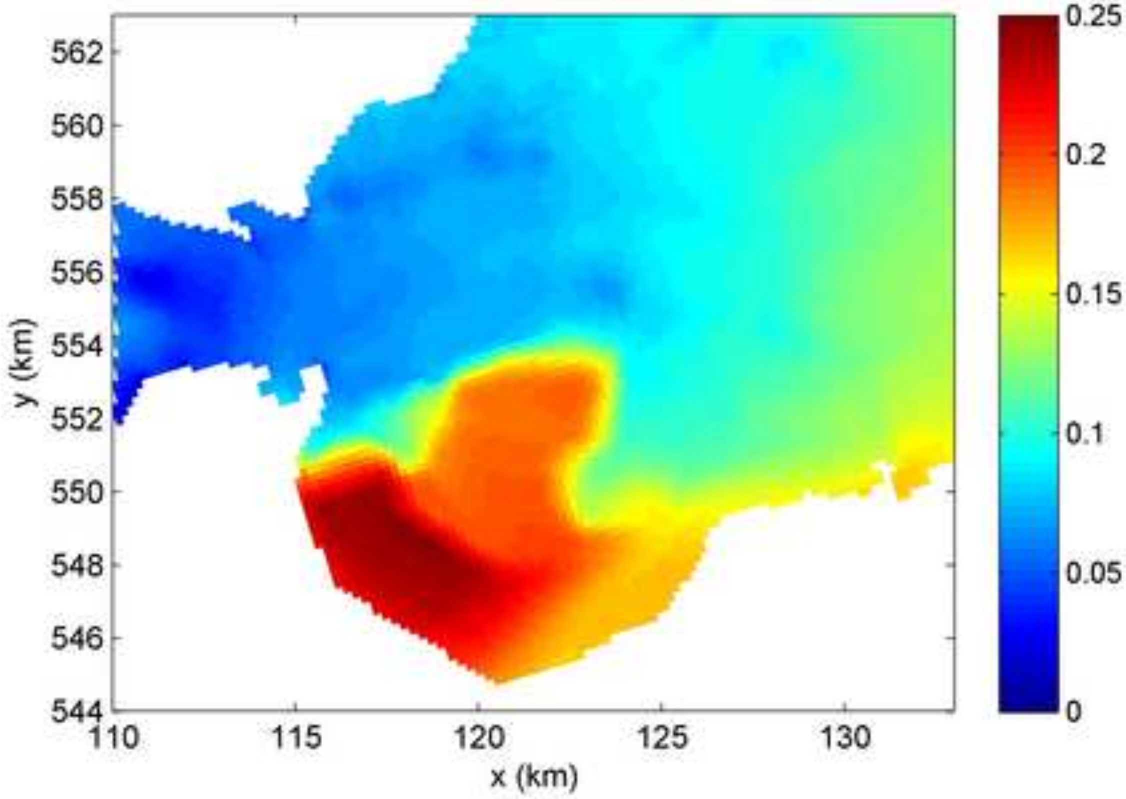

Figure(s)

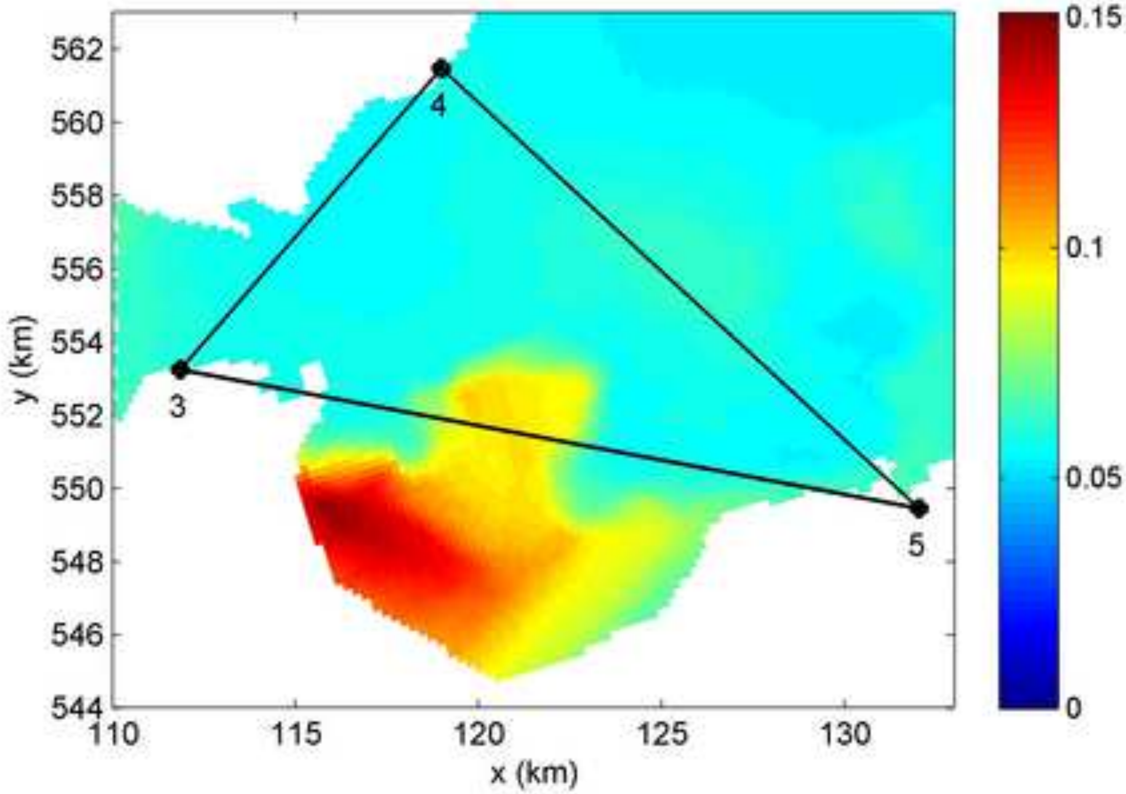
562
560
558
556
554
552
550
548
546
544
y (km)
110
115
120
125
130
x (km)
3
4
5
0.15
0.1
0.05
0

Figure(s)
Click here to download high resolution image

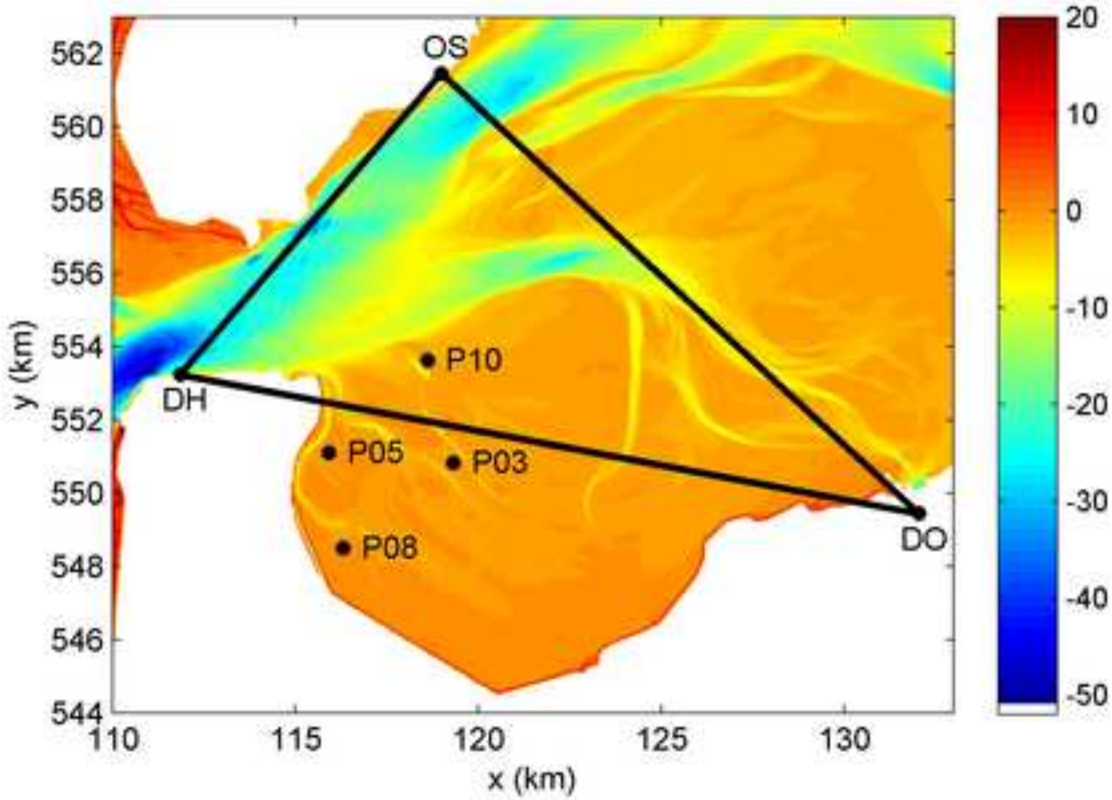

Figure(s)
Click here to download high resolution image

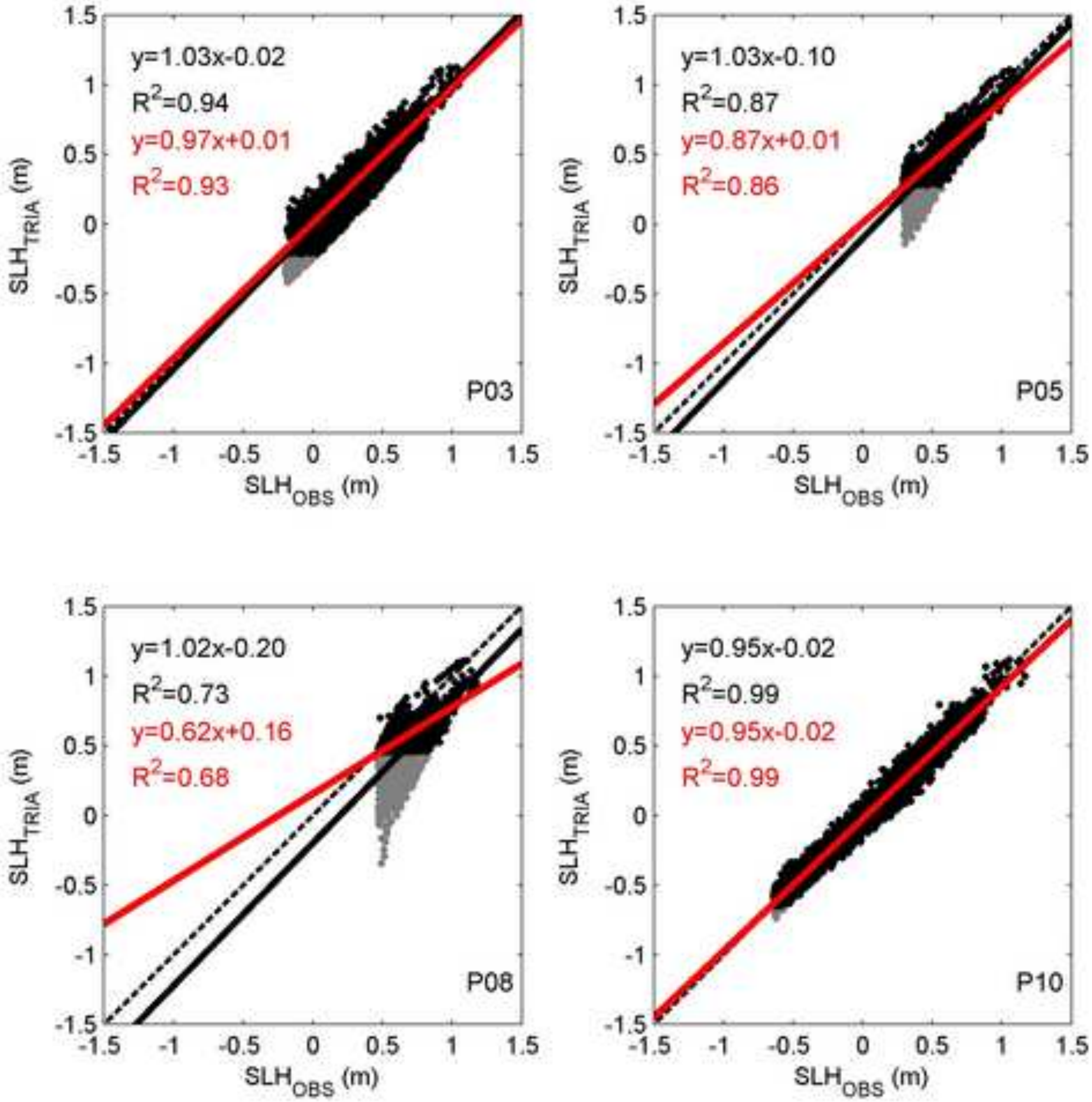

Figure(s)
Click here to download high resolution image

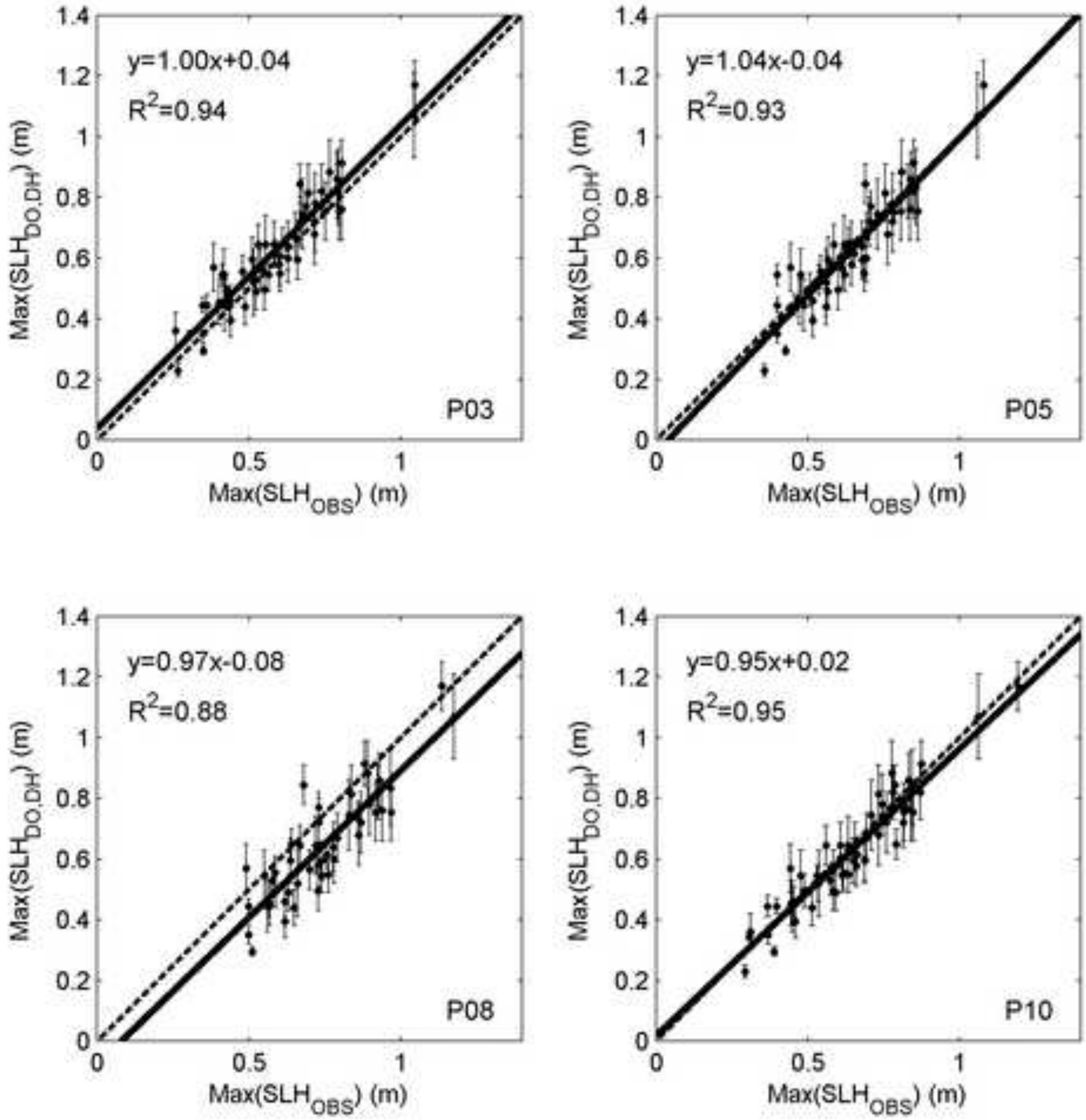

Figure(s)
Click here to download high resolution image

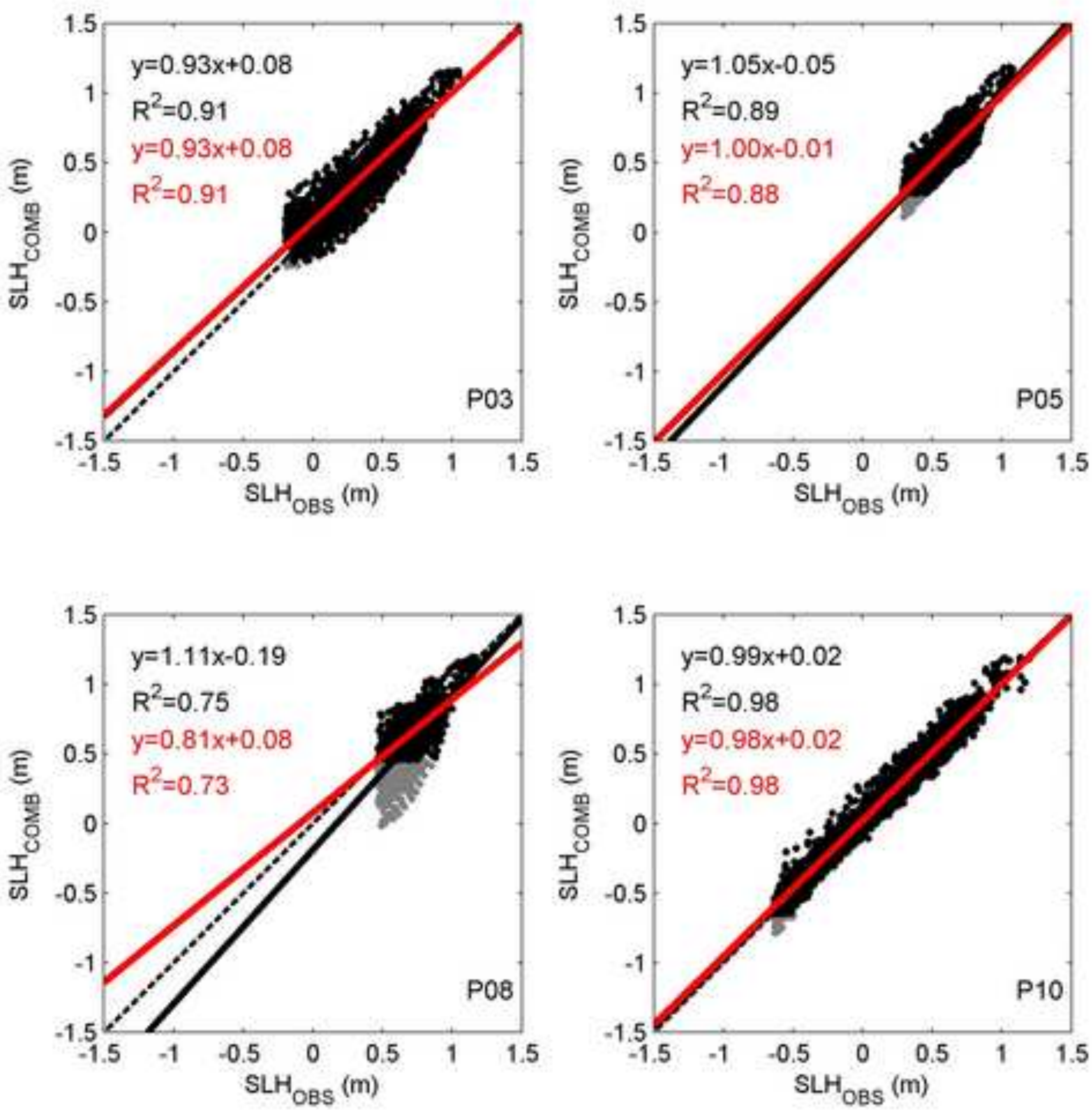

Figure(s)
[Click here to download high resolution image]

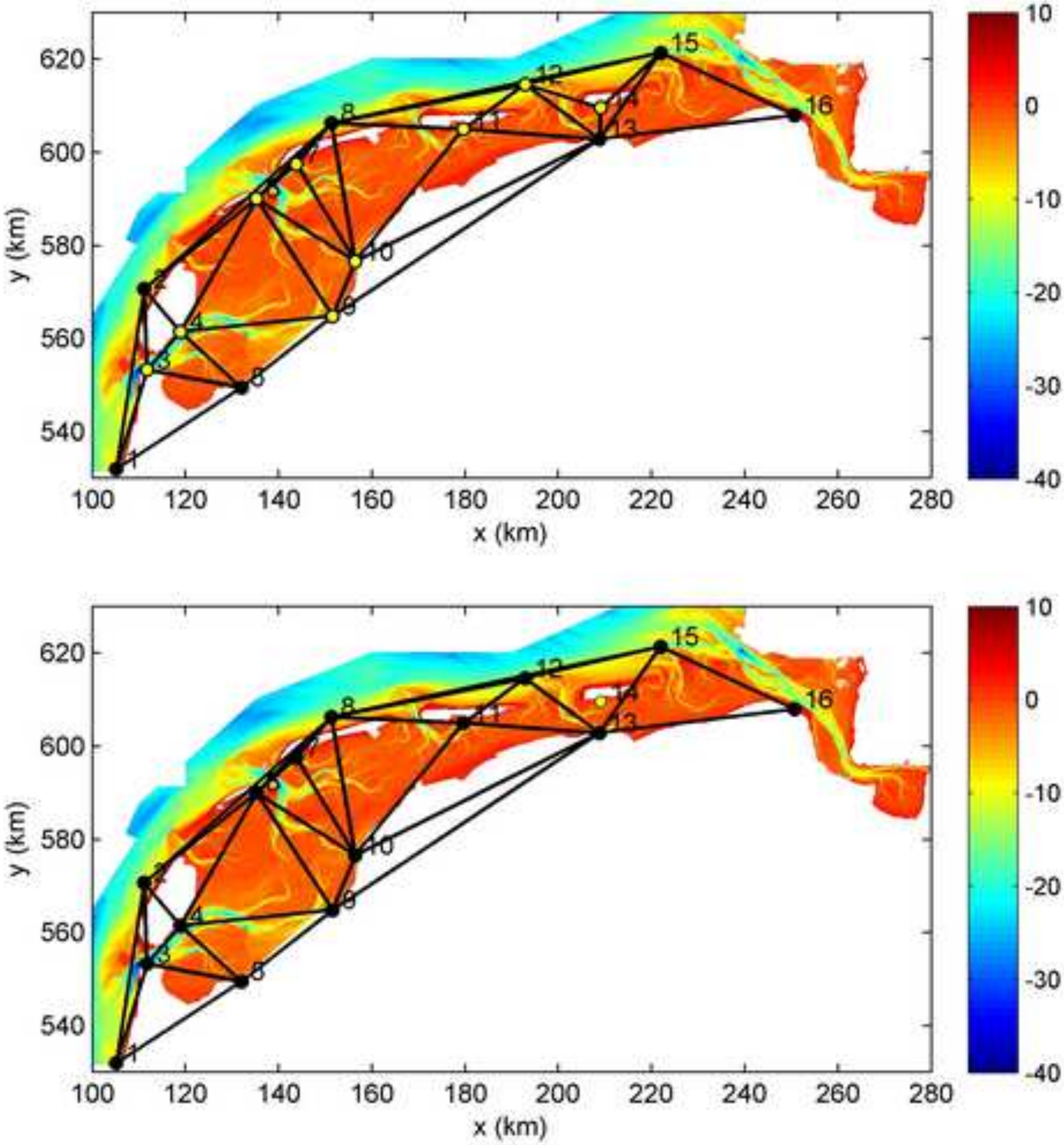

Figure(s)
Click here to download high resolution image